Available online at www.sciencedirect.com
ScienceDirect
Journal of Theoretical Biology 250 (2008) 322–338
Journal of Theoretical Biology
www.elsevier.com/locate/yjtbi

Adding self-renewal in committed erythroid progenitors improves the biological relevance of a mathematical model of erythropoiesis

Fabien Crauste[a,*], Laurent Pujo-Menjouet[a], Stéphane Génieys[a], Clément Molina[b], Olivier Gandrillon[b]

[a]*Université de Lyon, Université Lyon 1, CNRS, UMR 5208, Institut Camille Jordan, Bâtiment du Doyen Jean Braconnier, 43, blvd du 11 novembre 1918, F - 69222 Villeurbanne Cedex, France*

[b]*Equipe "Bases Moléculaires de l'Autorenouvellement et de ses Altérations," Université de Lyon, Université Lyon 1, Lyon, F-69003, France; CNRS, UMR5534, Centre de génétique moléculaire et cellulaire, Villeurbanne, F-69622, France*

Received 7 May 2007; received in revised form 21 September 2007; accepted 28 September 2007
Available online 6 October 2007

Abstract

We propose a new mathematical model of erythropoiesis that takes a positive feedback of erythrocytes on progenitor apoptosis into account, and incorporates a negative feedback of erythrocytes on progenitor self-renewal. The resulting model is a system of age-structured equations that reduces to a system of delay differential equations where the delays account for progenitor compartment duration and cell cycle length. We compare this model with experimental data on an induced-anemia in mice that exhibit damped oscillations of the hematocrit before it returns to equilibrium. When we assume no self-renewal of progenitors, we obtain an inaccurate fitting of the model with experimental data. Adding self-renewal in the progenitor compartment gives better approximations, with the main features of experimental data correctly fitted. Our results indicate the importance of progenitor self-renewal in the modelling of erythropoiesis. Moreover, the model makes testable predictions on the lifespan of erythrocytes confronted to a severe anemia, and on the progenitors behavior.

Keywords: Stress erythropoiesis; Self-renewal; Severe anemia; Age-structured model; Delay differential equations

1. Introduction

Hematopoiesis is the process through which all functional mature blood cells are generated. Homeostasis—that is the regulation of the production of different cell types to maintain stable populations—in the hematopoietic system is required in all vertebrates throughout life and needs a tight and constant regulation of decisions between proliferation, apoptosis and differentiation of hematopoietic cells.

All blood cells originate from hematopoietic stem cells (HSCs) (Weissman, 2000) entering differentiation pathways through successive divisions. Differentiated HSC form burst forming units (BFUs) and colony forming units (CFUs), known as progenitors. These latter can be separated in distinct lineages such as: white cells, platelets, or red blood cells. For example, differentiation of BFU-E and CFU-E can lead to the production of erythrocytes (red blood cells). Finally, after several divisions, progenitors become precursors. These latter go through a finite number of divisions before reaching the bloodstream as mature cells.

Self-renewal (Watt and Hogan, 2000) is the ability of a cell to divide and give two daughter cells that retain the same maturity as the mother cell, while keeping at all time the ability to engage in a differentiation process (i.e. to give two daughter cells, one of which at least being more mature than the mother cell). In the hematopoietic system, self-renewal is generally considered to be a specific property of the HSC (Weissman, 2000). However, neither the daily

*Corresponding author. Tel.: +33 472 448 516; fax: +33 472 431 687.
E-mail addresses: crauste@math.univ-lyon1.fr (F. Crauste), pujo@math.univ-lyon1.fr (L. Pujo-Menjouet), genieys@math.univ-lyon1.fr (S. Génieys), clmolina@laposte.net (C. Molina), Gandrillon@cgmc.univ-lyon1.fr (O. Gandrillon).

0022-5193/$ - see front matter © 2007 Elsevier Ltd. All rights reserved.
doi:10.1016/j.jtbi.2007.09.041

generation of 200×10^9 red blood cells nor stress erythropoiesis (Bauer et al., 1999) can easily be explained by the idea that only HSC can self-renew. Thus the hypothesis that immature progenitors can also self-renew has been proposed and has been supported by experimental evidences (Bauer et al., 1999; Gandrillon et al., 1999; Pain et al., 1991).

We focus our work here on erythropoiesis, the process through which red blood cells are produced. We explore the putative role of self-renewal at the progenitor level, through a mathematical modelling of erythropoiesis that can be confronted with real life data.

Numerous mathematical models of hematopoiesis or hematopoiesis lineages have been proposed (for a recent review, see Roeder, 2006). Among these, let us point out the work of Mackey (1978), who in 1978 published one of the pioneering paper in the field of physiological models for oscillating phenomena within the hematopoietic system. Mackey's model was based on publications by Lajtha (1959) and Burns and Tannock (1970).

Mackey's model has been developed then by many authors, including Mackey and co-workers, to describe differentiation and maturation processes involved in hematopoiesis more precisely. Bernard et al. (2003a, 2004) focused on the white blood cell production to bring an explanation to oscillatory behaviors observed in patients with cyclical neutropenia. Pujo-Menjouet and Mackey (2004) used a similar model to investigate the appearance of oscillations in blood cell counts within patients with chronic myelogenous leukemia. A global model was proposed by Colijn and Mackey (2005a, b), derived by combining sub-models of the various lineages, to explain some cases of periodic hematological diseases (see Haurie et al., 1998, 1999 for a review of periodic hematological diseases). The reader interested in the mathematical modelling of stem cells dynamics applied to blood diseases can consult Adimy and Crauste (2003), Adimy and Pujo-Menjouet (2003), Adimy et al. (2005a, b, 2006b), Mackey and Rudnicki (1994, 1999), Pujo-Menjouet et al. (2005) and the references therein.

In 1995, Bélair et al. (1995) proposed a modification of Mackey's model to consider the influence of growth factors on stem cell differentiation. The authors focused on erythropoiesis and assumed that erythropoietin (EPO)—a growth factor known to play a crucial role in erythropoiesis regulation—acted only on introduction of HSC in cycle. Their model was improved in 1998 by Mahaffy et al. (1998), and recently analyzed in detail by Ackleh et al. (2002, 2006) and Banks et al. (2004). Another erythropoiesis model, inspired by the same article, was introduced in Adimy et al. (2006a). In these works, EPO is the only growth factor supposed to act during erythropoiesis, and its action is always located at the introduction of HSCs in cell cycle. Recently, Adimy and Crauste (2007) considered a modification of the model in Bélair et al. (1995) to take the influence of erythropoietin on HSC apoptosis into account (Koury and Bondurant, 1990), but they only performed a theoretical study of the model.

An important contribution to mathematical modelling of erythropoiesis also appears in the works of Loeffler and his collaborators (Loeffler and Wichmann, 1980; Loeffler et al., 1989; Pantel et al., 1990; Wichmann and Loeffler, 1985; Wichmann et al., 1985, 1989; Wulff et al., 1989), mainly published between 1980 and 1990, but also recently (Roeder and Loeffler, 2002; Roeder, 2006). Throughout a collection of papers, Loeffler et al. investigate mathematical models of erythropoiesis and granulopoiesis, taking into account feedback controls from progenitors at the stem cell level and from mature cells (mainly assimilated to precursors) on progenitors. Their model also consider self-renewal of HSC. This is detailed in Wichmann and Loeffler (1985), where the authors investigated the behavior of this model, and fitted it to various experiments (including irradiations, bleeding, and phenylhydrazine treatments of mice). Application of their model to phenylhydrazine treatments can be compared to the results presented in Section 2, even though our experiments are closer to Wichmann and Loeffler experiments of bleeding on mice. However, all these works were performed, in particular, before the importance of EPO on the regulation of apoptosis was proved (Koury and Bondurant, 1990), and assumptions on erythroid progenitor self-renewal appeared (Bauer et al., 1999; Gandrillon et al., 1999; Pain et al., 1991). Moreover, the dynamics observed by the authors in their series of erythropoiesis–granulopoiesis modelling works is mainly concerned with hematopoietic stem cells properties and their regulation, and this latter problem is still only partially known at the molecular level (Krause, 2002).

In this work, we modify the erythropoiesis part of Colijn and Mackey's 2005a model in order to focus ourselves on the influence of EPO upon progenitor apoptosis (Koury and Bondurant, 1990) and of glucocorticoids upon progenitor self-renewal (Bauer et al., 1999). Indeed, Colijn and Mackey (2005a) only considered feedback of the erythrocyte population on the rate of differentiation of HSCs, and no self-renewal appears elsewhere but in the HSCs compartment. To the best of our knowledge, the latter assumption on the feedback control of erythrocytes on HSCs differentiation is no longer believed to hold amongst biologists (see Krause, 2002). We first present some experimental results that seem to indicate the importance of self-renewal for progenitors. Then, we propose a new model for erythropoiesis, which is an age-structured model, that we reduce to a system of delay differential equations (similarly to what has been done by Bélair et al., 1995). We then analyze this model without taking self-renewal into account, in Section 5, and show that, even though theoretical results display interesting properties, the model does not fit experimental data well. After carrying out numerical simulations on the complete model, we conclude in Section 6 that progenitor self-renewal in erythropoiesis is important, as expected from experimental data. In the last section, a discussion stresses out the limits of this model and rises new questions concerning erythropoiesis modelling.

2. Experimental evidence of feedback controls

In order to study the kinetics of erythrocyte populations, we performed a series of experiments (in the Centre de Génétique Moléculaire et Cellulaire Laboratory, O. Gandrillon's team) to measure hematocrit in mice. Hematocrit is a test that measures the volume of red blood cells in a blood sample. It gives a percentage of erythrocyte volume found in the whole blood system. It can be considered that a blood sample is mainly composed with erythrocytes and plasma, since platelets and white cells volumes can be easily neglected. Our approach consisted in destabilizing the steady state hematocrit by creating an anemia, and observing the return to equilibrium.

The hematocrit values were taken from two different batches of adult outbred Hsd-ICR mice. Each batch consisted of six males and six females. One batch was rendered anemic by two intraperitoneal phenylhydrazine injections (60 mg/kg body weight) at 24 h intervals. The control batch was not injected. Blood was collected from the peri-orbital sinus of the mouse directly in microhematocrit tubes at the indicated time intervals (that is daily intervals excluding Sundays for 2 weeks and then at 2–3 days intervals for the rest of the period, for the anemic batch, and at 2–3 days intervals for the control batch). Fig. 1 shows the results of this experiment.

The hematocrit of the control batch stays at its steady value, between 45% and 50% (Panel B), whereas the hematocrit of the injected batch (Panel A) displays very clear features: following the anemia, that makes the hematocrit fall to very low values (about $23 \pm 3\%$), the hematocrit rapidly increases to reach a high value (about $55 \pm 3\%$), and then returns to the equilibrium, but not in a very smooth manner.

In both cases, it seems that the hematocrit oscillates about its steady value. However, the standard deviation lines in the hematocrit of the control batch (Fig. 1B) seem to indicate that what could be thought as oscillations corresponds in fact to perturbations about the mean. For the anemia-induced batch, however, anemia seems to trigger damped oscillations before the hematocrit returns to the equilibrium.

A simple way to determine periodicity in unevenly distributed data samples is to use the Lomb periodogram (Lomb, 1976). If a periodicity exists in a data sample, then it corresponds to a peak in the periodogram curve. We computed the Lomb periodogram for the data in Fig. 1 (data not shown here), and they tend to corroborate the above remark on the damped oscillations. However, since we do not really look for any periodicity in our data, but rather for damped oscillations, the use of the Lomb periodogram can be discussed. One can however keep in mind that the Lomb periodogram confirms that a normal hematocrit does not oscillate.

In the next section, we propose a new model for erythropoiesis, that incorporates nonlinear apoptosis and self-renewal rates of progenitors. This model will be confronted to the above experimental data corresponding to a severe anemia, in order to stress the importance of erythroid progenitors self-renewal in erythropoiesis.

3. An age-structured model of erythropoiesis

As described in the introduction, one can basically consider that erythropoiesis involves three types of cell populations. HSCs, considered as the root of the process, progenitors also known as committed stem cells coming from differentiated HSCs, and erythrocytes, or red blood cells, which are the final state of cells in erythropoiesis.

The question of the control of HSC differentiation into given lineages is open (see e.g. Krause, 2002 for a review). It is especially unclear to see whether this cell fate decision is controlled by a purely stochastic mechanism or is the result of environmental cues mediated at least in part through specific receptor ligand interactions. Since this part of the process is mostly unknown, and since we are interested in modelling the erythroid progenitor compartment, we decided not to incorporate the control of HSC

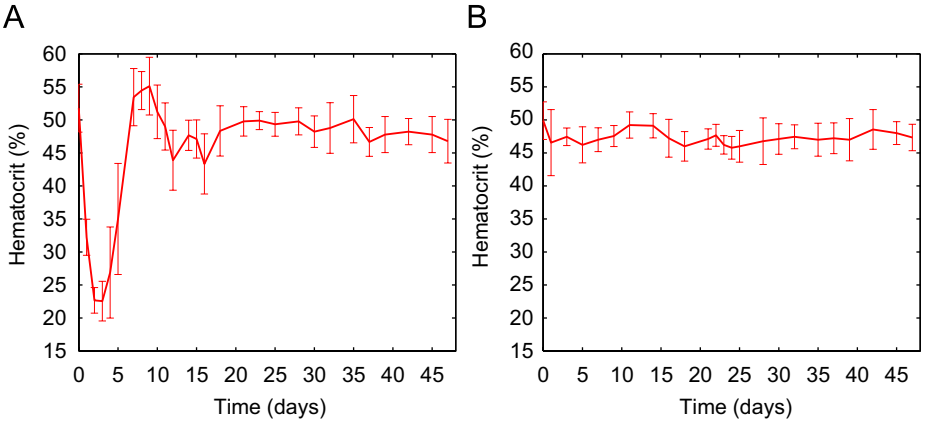

Fig. 1. Hematocrit values from two different batches of adult outbred Hsd-ICR mice, over 48 days. Average hematocrit is represented, with standard deviation lines on either side of the mean. Panel A: Hematocrit of the anemic batch (injected with phenylhydrazine). Panel B: Hematocrit of the control batch (not injected).

differentiation in the model, but to model the flow from HSC into erythroid progenitor as a constant. Hence, in our model, we do not consider the HSC population but rather the influx of HSC becoming progenitors, denoted by K.

Then, let us consider three different cell populations, self-renewing progenitors, non-self-renewing progenitors and erythrocytes, with densities respectively denoted by $p_{sr}(t,a)$, $p(t,a)$ and $e(t,a)$. These quantities represent the densities of cell populations formed by progenitors (for $p_{sr}(t,a)$ and $p(t,a)$) or erythrocytes (for $e(t,a)$) with age a at time t. For progenitors, age corresponds to the time spent between two successive divisions. It can be noted that all cells age with unitary velocity, that is

$$\frac{\mathrm{d}a}{\mathrm{d}t}=1.$$

Dynamics of these populations are as follows. The progenitor compartment is supplied at a constant rate K with HSCs. Progenitors die by apoptosis with a rate β and they self-renew with a rate σ. We denote by τ_c the time needed by a progenitor to self-renew, and by τ_p the progenitor compartment duration, that is the time needed by a progenitor cell to become mature and enter the last part of its differentiation process. Self-renewing progenitors can also die by apoptosis. After maturing and differentiating, progenitors become erythrocytes—we do not explicitly take progenitor differentiation through divisions into account, but we suppose that the cell population entering the erythrocyte compartment corresponds to the progenitors at the end of their compartment (that is when $t=\tau_p$), multiplied by an amplification parameter A which describes the successive divisions of progenitors (about 7–8 divisions). Erythrocytes are assumed to die with a constant rate γ, equal to 1 over the average lifespan of an erythrocyte. They modulate apoptosis and self-renewal of progenitors through control loops. Erythrocytes are assumed to positively control apoptosis of progenitors, and negatively control their self-renewal. A schematic representation of this model is provided in Fig. 2.

Then, densities $p(t,a)$, $p_{sr}(t,a)$ and $e(t,a)$ satisfy the following evolution equations for $t,a>0$:

$$\frac{\partial p}{\partial t}(t,a)+\frac{\partial p}{\partial a}(t,a)=-\beta p(t,a)-\sigma p(t,a),$$

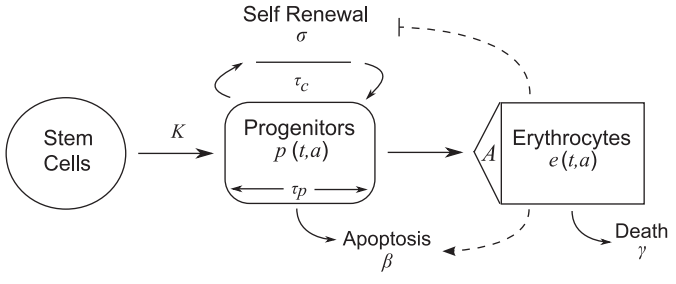

Fig. 2. Schematic representation of the model. Progenitors have an ability to self-renew. A negative feedback of erythrocytes on this self-renewal is incorporated, as well as a positive feedback on progenitor apoptosis. Dashed lines indicate feedback controls.

$$\frac{\partial p_{sr}}{\partial t}(t,a)+\frac{\partial p_{sr}}{\partial a}(t,a)=-\beta p_{sr}(t,a),$$
$$\frac{\partial e}{\partial t}(t,a)+\frac{\partial e}{\partial a}(t,a)=-\gamma e(t,a). \quad (1)$$

This system must be completed by boundary conditions, describing the cell flux between the three compartments (progenitors, self-renewing progenitors and erythrocytes), and initial conditions representing an initial distribution of populations in the system. We do not pay too much attention to initial conditions because our next step will be to reduce system (1) to a delay differential system with different initial conditions.

Boundary conditions for system (1) are given by

$$p(t,0)=K+2p_{sr}(t,\tau_c),$$
$$p_{sr}(t,0)=\int_0^{\tau_p}\sigma p(t,a)\,\mathrm{d}a,$$
$$e(t,0)=Ap(t,\tau_p). \quad (2)$$

The first condition in (2) describes the input of progenitors. Cells entering the progenitor compartment come from HSCs (that is K) and from self-renewing progenitors that have completed a cell cycle ($2p_{sr}(t,\tau_c)$). The second equation represents progenitors entering self-renewal. The third equation describes new erythrocytes coming from the progenitor compartment.

We do not impose a maximal age for erythrocytes, but we assume

$$\lim_{a\to+\infty} e(t,a)=0$$

fast enough for the total density of erythrocytes $\int_0^{+\infty} e(t,a)\mathrm{d}a$ to be finite for all time t.

We assume that erythrocytes apply a positive feedback on progenitor apoptosis, and a negative feedback on progenitor self-renewal. In fact, progenitor apoptosis is mainly mediated by EPO, whose production is in turn dependent on the number of circulating erythrocytes. We do not want, for the moment, to complicate our erythropoiesis modelling by adding EPO concentration. So we implicitly describe its influence on apoptosis by considering that apoptosis depends on the total number of erythrocytes. In the same way, self-renewal seems to be mainly mediated by glucocorticoids (cortisol), but we suppose that self-renewal depends only on the total number of erythrocytes. That is, we assume

$$\beta=\beta\left(\int_0^{+\infty}e(t,a)\,\mathrm{d}a\right)\quad\text{and}\quad\sigma=\sigma\left(\int_0^{+\infty}e(t,a)\,\mathrm{d}a\right),$$

where β is a positive, continuous and increasing function, with

$$\beta(0)=0\quad\text{and}\quad\lim_{E\to+\infty}\beta(E)=\beta_\infty>0,$$

and σ a positive, continuous and decreasing function, with

$$\sigma(0)=\sigma_0>0\quad\text{and}\quad\lim_{E\to+\infty}\sigma(E)=0.$$

Under these assumptions, system (1)–(2) is nonlinear, with positive and negative controls. In the next section, we show that this model can be easily reduced to a system of two nonlinear differential equations with delays.

4. Reduction to a system of delay differential equations

Let us define the total densities of non-self-renewing progenitors, self-renewing progenitors and erythrocytes at time t, denoted by $P(t)$, $P_{sr}(t)$ and $E(t)$, respectively, as

$$P(t)=\int_0^{\tau_p} p(t,a)\,\mathrm{d}a,$$
$$P_{sr}(t)=\int_0^{\tau_c} p_{sr}(t,a)\,\mathrm{d}a \quad \text{and} \quad E(t)=\int_0^{+\infty} e(t,a)\,\mathrm{d}a.$$

Integrating system (1) over the age (between $a=0$ and $a=\tau_p$ for $p(t,a)$, $a=0$ and $a=\tau_c$ for $p_{sr}(t,a)$, and $a=0$ and $a=+\infty$ for $e(t,a)$), one obtains

$$\frac{\mathrm{d}P}{\mathrm{d}t}(t)=-[\beta(E(t))+\sigma(E(t))]P(t)+p(t,0)-p(t,\tau_p),$$
$$\frac{\mathrm{d}P_{sr}}{\mathrm{d}t}(t)=-\beta(E(t))P_{sr}(t)+p_{sr}(t,0)-p_{sr}(t,\tau_c),$$
$$\frac{\mathrm{d}E}{\mathrm{d}t}(t)=-\gamma E(t)+e(t,0),$$

which becomes, using (2),

$$\begin{aligned}\frac{\mathrm{d}P}{\mathrm{d}t}(t)=&-[\beta(E(t))+\sigma(E(t))]P(t)\\&+K+2p_{sr}(t,\tau_c)-p(t,\tau_p),\\\frac{\mathrm{d}P_{sr}}{\mathrm{d}t}(t)=&-\beta(E(t))P_{sr}(t)\\&+\sigma(E(t))P(t)-p_{sr}(t,\tau_c),\\\frac{\mathrm{d}E}{\mathrm{d}t}(t)=&-\gamma E(t)+Ap(t,\tau_p).\end{aligned}\tag{3}$$

One needs to determine $p_{sr}(t,\tau_c)$ and $p(t,\tau_p)$ to obtain a clear expression for system (3). To that aim, we use the method of the characteristics (see Appendix A for details). We thus obtain, for $t>\tau_p+\tau_c$, the reduced model

$$\begin{aligned}\frac{\mathrm{d}P}{\mathrm{d}t}(t)=&-[\beta(E(t))+\sigma(E(t))]P(t)\\&+K+2\sigma(E(t-\tau_c))P(t-\tau_c)\\&\times\exp\left(-\int_{t-\tau_c}^{t}\beta(E(s))\,\mathrm{d}s\right)\\&-\left[K+2\sigma(E(t-\tau_p-\tau_c))P(t-\tau_p-\tau_c)\right.\\&\left.\times\ \exp\left(-\int_{t-\tau_p-\tau_c}^{t-\tau_p}\beta(E(s))\,\mathrm{d}s\right)\right]\\&\times\exp\left(-\int_{t-\tau_p}^{t}(\beta(E(s))+\sigma(E(s)))\,\mathrm{d}s\right),\\\frac{\mathrm{d}E}{\mathrm{d}t}(t)=&-\gamma E(t)+A\exp\left(-\int_{t-\tau_p}^{t}(\beta(E(s))+\sigma(E(s)))\,\mathrm{d}s\right)\\&\times\left[K+2\sigma(E(t-\tau_p-\tau_c))P(t-\tau_p-\tau_c)\right.\\&\left.\times\ \exp\left(-\int_{t-\tau_p-\tau_c}^{t-\tau_p}\beta(E(s))\,\mathrm{d}s\right)\right],\end{aligned}\tag{4}$$

where the equation for P_{sr} is omitted since it has no impact on other equations of (4). However, introducing the population of self-renewing progenitors was convenient to obtain system (4) as shown in Appendix A.

Let us briefly explain the role of each term in system (4).

The first equation describes the evolution of the total density of progenitors. The first terms on the right-hand side of the first equation account for cell loss due to apoptosis and cells entering self-renewal. The second term represents the amount of cells entering the progenitor compartment, one part from the HSC compartment and the other one from cells that have completed a cell cycle and re-entered the progenitor compartment (self-renewal), after division (that is why there is a coefficient 2). Finally, the last term is for progenitors that become erythrocytes (one can note that some of these cells directly derive from HSCs that have survived the progenitor compartment).

The second equation determines the evolution of the erythrocyte density. Erythrocytes can only die, with a constant rate γ, and the second term in the right-hand side of the second equation is for progenitors that enter the erythrocyte compartment, as described above.

In the next sections, we investigate this model, first without self-renewal and then with it. Then we point out the main differences between these two cases.

5. Is it necessary to take self-renewal of progenitors into account to reproduce experimental results?

Before investigating the dynamics of system (4) and the consequences of apoptosis and self-renewal, let us first consider the case where progenitors do not self-renew. Then the erythropoiesis process, as described in Fig. 2, becomes simpler as shown in Fig. 3.

In this case, system (4) becomes

$$\frac{\mathrm{d}P}{\mathrm{d}t}(t)=-\beta(E(t))P(t)+K\left[1-\exp\left(-\int_{t-\tau_p}^{t}\beta(E(s))\,\mathrm{d}s\right)\right],\tag{5}$$

$$\frac{\mathrm{d}E}{\mathrm{d}t}(t)=-\gamma E(t)+AK\exp\left(-\int_{t-\tau_p}^{t}\beta(E(s))\,\mathrm{d}s\right).\tag{6}$$

This is an uncoupled system of nonlinear differential equations with a single delay τ_p. The important point is that Eq. (6) does not depend on the progenitor population $P(t)$. Hence, it is sufficient to focus on the dynamics of the

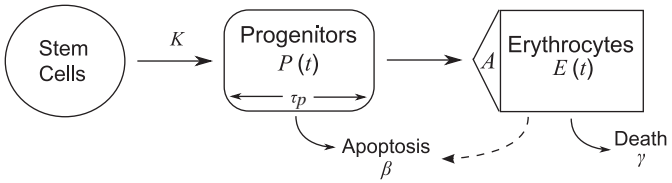

Fig. 3. A schematic representation of erythropoiesis without progenitor self-renewal. We consider two cell populations, progenitors $P(t)$ and erythrocytes $E(t)$. Details of the considered mechanisms describing the dynamics of progenitor and erythrocyte populations are given in Section 3, except that there is no progenitor self-renewal in the present case. Erythrocytes positively control progenitor apoptosis (dashed line).

solutions of Eq. (6). In particular, one only needs to determine a steady state of (6) and its asymptotic behavior to deduce the asymptotic behavior of the entire system (5)–(6).

Even though self-renewal of erythroid progenitors can be considered as the main feature of system (4), it is not the only novelty incorporated in this system. In particular, the feedback control of erythrocytes (via EPO, even in an implicit way) on progenitors apoptosis has never been used in erythropoiesis modelling (the only feedback on apoptosis considered in previous studies used to have an influence on the HSC population, see Adimy and Crauste, 2007), so system (5)–(6) does not reduce to any previously published model of erythropoiesis.

We recall that the apoptosis function $E\mapsto\beta(E)$ is assumed to be increasing with

$$\beta(0)=0 \quad \text{and} \quad \lim_{E\to\infty}\beta(E)=\beta_\infty>0.$$

We first concentrate on the existence of steady states for system (5)–(6). We investigate then the stability of this steady state and we focus on numerical simulations.

5.1. Existence of steady states

We recall that (P^*,E^*) is a steady state of system (5)–(6) if P^* and E^* are solutions of (5)–(6) satisfying

$$\frac{\mathrm{d}P^*}{\mathrm{d}t}(t)=\frac{\mathrm{d}E^*}{\mathrm{d}t}(t)=0 \quad \text{for } t>0.$$

Consequently, a steady state of system (5)–(6), also called a stationary solution or equilibrium, is a constant solution of (5)–(6).

Thus, a steady state (P^*,E^*) of system (5)–(6) satisfies

$$\beta(E^*)P^*=K[1-\mathrm{e}^{-\tau_p\beta(E^*)}], \tag{7}$$

$$\gamma E^*=AK\mathrm{e}^{-\tau_p\beta(E^*)}. \tag{8}$$

Eq. (8) gives the existence of a unique $E^*>0$ satisfying (8). Indeed, since β is a positive and increasing function, the mapping $z\mapsto AK\mathrm{e}^{-\tau_p\beta(z)}$ is decreasing for $z\geqslant 0$, and ranges from AK to $AK\mathrm{e}^{-\tau_p\beta_\infty}$. The function $z\mapsto\gamma z$ is strictly increasing and ranges from 0 to $+\infty$. Therefore, we deduce the existence of a unique $E^*>0$ verifying (8).

From the expression of E^* one easily deduces P^* using (7), that is

$$P^*=K\frac{1-\mathrm{e}^{-\tau_p\beta(E^*)}}{\beta(E^*)}=\frac{AK-\gamma E^*}{A\beta(E^*)}.$$

Thus we claim the existence of a unique steady state (P^*,E^*) of system (5)–(6) defined by (7)–(8), and satisfying

$$\frac{AK\mathrm{e}^{-\tau_p\beta_\infty}}{\gamma}<E^*<\frac{AK}{\gamma} \quad \text{and} \quad 0<P^*<K\frac{1-\mathrm{e}^{-\tau_p\beta_\infty}}{\beta(AK\mathrm{e}^{-\tau_p\beta_\infty}/\gamma)}. \tag{9}$$

From a biological point of view, the quantity AK/γ corresponds to the steady state value of the erythrocyte density in the absence of progenitor apoptosis (it is easily seen from (8) with $\beta=0$), and similarly $AK\mathrm{e}^{-\tau_p\beta_\infty}/\gamma$ corresponds to the steady state value when apoptosis is at its maximum. Thus the above inequality on E^* only gives bounds for E^* that correspond to extreme situations in system (7)–(8), these bounds describing absolutely virtual erythrocyte densities.

5.2. Asymptotic stability and existence of periodic solutions

We analyze the asymptotic behavior of the unique steady state of system (5)–(6) by linearizing it about its steady state. Since the behavior of system (5)–(6) is entirely given by the behavior of the solution $E(t)$, we only linearize Eq. (6) about E^*.

We set $z(t)=E(t)-E^*$. Then Eq. (6) linearized about E^* is

$$\frac{\mathrm{d}z}{\mathrm{d}t}(t)=-\gamma z(t)-\xi\int_{-\tau_p}^{0}z(t+s)\,\mathrm{d}s, \tag{10}$$

where, from (8),

$$\xi=AK\beta'(E^*)\mathrm{e}^{-\tau_p\beta(E^*)}=\gamma E^*\beta'(E^*)>0. \tag{11}$$

From Eq. (10) we can deduce the characteristic equation of (6), defined by

$$\lambda+\gamma+\xi\int_{-\tau_p}^{0}\mathrm{e}^{\lambda s}\,\mathrm{d}s=0, \quad \lambda\in\mathbb{C}. \tag{12}$$

By studying the complex roots of (12), that are called characteristic roots of (10) or eigenvalues, we can determine whether E^* is asymptotically stable or unstable.

The asymptotic stability of E^* is determined by the sign of the real parts of eigenvalues of (10), that is of roots of (12). If all eigenvalues of (10) have negative real parts, then E^* is locally asymptotically stable. If there exist eigenvalues of (10) with positive real parts, then E^* is unstable. Moreover, the stability of E^* can only be lost if purely imaginary eigenvalues appear.

We first check (see Appendix B for details) that $\lambda=0$ is not an eigenvalue of (10), so the integral in (12) can be computed and (12) is equivalent to

$$\lambda^2+\gamma\lambda+\xi-\xi\,\mathrm{e}^{-\lambda\tau_p}=0 \quad \text{and} \quad \lambda\neq 0.$$

The study of complex roots of (12) is then equivalent to the study of non-zero complex roots of

$$\lambda^2+\gamma\lambda+\xi-\xi\,\mathrm{e}^{-\lambda\tau_p}=0. \tag{13}$$

It is straightforward (see Appendix B) to obtain that all non-zero roots of (13) have negative real parts when $\tau_p=0$, that is E^* is locally asymptotically stable in this case.

Consequently, we check if there could exist a critical value of $\tau_p>0$ that destabilizes the steady state E^*. Actually, we are going to prove that the steady state may be destabilized through a Hopf bifurcation (see details in Appendix B).

Assuming $\tau_p>0$, and looking for eigenvalues of the form $\lambda=\mathrm{i}\omega$, with $\omega\in\mathbb{R}$, we first obtain that (10) has no purely imaginary characteristic roots if $2\xi\leqslant\gamma^2$, and so the stability of the steady state E^* cannot be modified. Since it is locally asymptotically stable when $\tau_p=0$, then it is locally asymptotically stable for $\tau_p\geqslant 0$ under condition $2\xi\leqslant\gamma^2$.

Then, studying the case $2\xi>\gamma^2$, using simple techniques (see, for example, Kuang, 1993) one obtains the existence of simple purely imaginary roots $\pm\mathrm{i}\omega$ of (10), with $\omega=\sqrt{2\xi-\gamma^2}$, for

$$\tau_p=\tau_p^*:=\frac{\arccos\left(\dfrac{\gamma^2}{\xi}-1\right)}{\sqrt{2\xi-\gamma^2}}.$$

Moreover, these characteristic roots satisfy the so-called *transversality condition*, that is real parts of the branch of eigenvalues that passes through $\pm\mathrm{i}\sqrt{2\xi-\gamma^2}$ cross the horizontal axis. This property is necessary to establish the existence of a Hopf bifurcation at the steady state for $\tau_p=\tau_p^*$.

We can then conclude to the following proposition, which summarizes the behavior of the unique steady state of system (5)–(6).

Proposition 1. *If $2\xi>\gamma^2$, then for $0\leqslant\tau_p<\tau_p^*$, the steady state E^* is locally asymptotically stable and, for $\tau_p\geqslant\tau_p^*$ it is unstable. When $\tau_p=\tau_p^*$ a Hopf bifurcation occurs at E^* and periodic solutions appear.*

If $2\xi\leqslant\gamma^2$, the steady state E^* is locally asymptotically stable for all $\tau_p\geqslant 0$.

According to the result in Proposition 1, the erythropoiesis process can theoretically lead to the appearance of periodic solutions of the circulating erythrocyte number—through a Hopf bifurcation—and therefore damped oscillations should be observed before the bifurcation, when the steady state is about to be destabilized.

5.3. Numerical simulations

We are interested in modelling the rapid recovery of the level of erythrocytes observed after acute anemia (see Section 2). To that aim, we compute the solution $E(t)$ of (6), using the MATLAB solver dde23 which allows the numerical resolution of delay differential equations (Shampine and Thompson, 2001), and we use this solution to draw the hematocrit corresponding to our simulation.

The hematocrit $H(t)$ is defined by

$$H(t)=\frac{vE(t)}{vE(t)+\text{plasma volume}},$$

where v is the considered volume per mass density unit of the erythrocytes. Assuming plasma volume is not modified by our experimental induction of anemia, we relate it to the steady hematocrit, denoted by H^* (with H^* about 45–50%, see Fig. 1), and the steady state E^*. Since, at the steady state,

$$H(t)=H^*=\frac{vE^*}{vE^*+\text{plasma volume}},$$

we deduce that

$$\text{plasma volume}=\frac{1-H^*}{H^*}vE^*.$$

Consequently, in the following, we assume that the hematocrit is given by

$$H(t)=\frac{E(t)}{E(t)+(1-H^*)E^*/H^*}.$$

Taking the inverse function, we have

$$E(t)=\frac{H(t)}{1-H(t)}\quad\frac{1-H^*}{H^*}E^*. \tag{14}$$

We compute E^* from Eq. (6), and H^* from the experimental curve in Fig. 1.

Since $E(t)$ is the solution of a delay differential equation, an initial condition for Eq. (6) must be supplied on the interval $[-\tau_p,0]$. We consider, as an initial condition for our problem, the function that describes a strong decay of the hematocrit from H^* to H_{min}, on the interval $[-\tau_{in},0]$ (here, according to Fig. 1, $\tau_{in}=3$ days). It follows that the initial condition for $H(t)$ in this case is

$$H_0(t)=\begin{cases}H^*, & \text{for } t\in[-\tau_p,-\tau_{in}],\\ \dfrac{H^*-H_{min}}{\tau_{in}^*}t+H_{min}, & \text{for } t\in[-\tau_{in},0].\end{cases}$$

Using (14), we choose as initial condition for Eq. (6)

$$E_0(t)=E^*\frac{1-H^*}{H^*}\times\frac{H_0(t)}{1-H_0(t)},\quad \text{for } t\in[-\tau_p,0]. \tag{15}$$

Using this initial condition for Eq. (6), we hope to obtain a description of the rapid increase of the hematocrit, with a significant peak and damped oscillations before a steady hematocrit.

In Table 1, values of the parameters used in the simulations are listed. We discuss hereafter these values.

The hematopoietic stem cell influx is known to be, in mammals, about $10^4\,\text{cells}\,(\text{gd})^{-1}$, at maximum. We suppose here that $K=10^4\,\text{cells}\,(\text{gd})^{-1}$, even if it can be varied between 10^3 and $10^4\,\text{cells}\,(\text{gd})^{-1}$. The death rate of erythrocytes, estimated by considering that the average

Table 1
Table of parameters

Parameters		Values used	Range
γ	Erythrocytes mortality rate (d^{-1})	0.025	–
A	Amplification parameter	2^8	$2^4 - 2^8$
K	HSC population density entering the progenitor compartment per day (cells $(gd)^{-1}$)	10^4	$10^3 - 10^4$
τ_p	Progenitor compartment duration (days)	4	–
τ_c	Self-renewal cycle duration (days)	1	–
β_∞	Maximum apoptosis rate (d^{-1})	1	0.5 – 1
$\overline{\beta}$	Threshold value of the apoptosis rate (cells d^{-1})	10^7 [a], 10^8	$10^7 - 10^9$
n	Sensitivity of the apoptosis rate	8	–
σ_0	Maximum self-renewal rate (d^{-1})	0.5	–
$\overline{\sigma}$	Threshold value of the self-renewal rate (cells d^{-1})	10^9	$10^6 - 10^{10}$
m	Sensitivity of the self-renewal rate	5	–

Values of the different parameters involved in system (4) are listed in two columns: in the first one, values used in simulations with and without taking self-renewal into account, and in the second column a range for each parameter, when available.
[a]This value is only used in the absence of self-renewal.

erythrocyte life in mice is 40 days, is taken to be $\gamma = 1/40 = 0.025\,d^{-1}$. The amplification parameter A should correspond to a range of 4–8 divisions, with mortality of some cells. We consider that A varies between 2^4 and 2^8, and we usually use the value $A = 2^8$. The progenitor compartment duration τ_p is chosen by considering that progenitors need about four divisions to differentiate into precursor cells. Therefore we choose $\tau_p =$ 4 days.

The apoptosis rate $\beta(E)$ is chosen as a Michaelis–Menten function,

$$\beta(E) = \beta_\infty \frac{E^n}{E^n + \overline{\beta}^n}.$$

The parameter n describes the sensitivity of the apoptosis rate, β_∞ is the maximum apoptosis rate, and $\overline{\beta}$ the value of erythrocyte density for which the apoptosis rate attains half of its maximum.

The shape of the apoptosis rate function can be deduced from Chappell et al. (1997), where the viability dose response of cells to EPO is presented, and Sakata et al. (1985), where the relation between EPO concentration and mature erythrocytes density (via hemoglobin concentration) is described. This led to the Michaelis–Menten function given above to describe the implicit dependence of apoptosis on mature erythrocytes. It can be noted that, to our knowledge, only one work (Adimy and Crauste, 2007) considered an erythropoiesis model with a feedback control of apoptosis, but the feedback function was different, since EPO concentration was explicitly incorporated in the model, which is not the case in the present study.

All the coefficients of the apoptosis function β are rather difficult to estimate. Usually, apoptosis in mice varies between 2% and 50%. So we could be tempted to take β_∞ equals to 0.5. However, since β_∞ represents the maximum apoptosis rate, and since it is a limit value in the function $\beta(E)$, we could also take $\beta_\infty = 1$. It is difficult to choose a good value for $\overline{\beta}$. Since the maximum apoptosis rate is not exactly known, it is not easy to determine the value for which half of this maximum is reached. We decided to fix $\overline{\beta}$ in the range of the erythrocyte density level at equilibrium, that is between 10^7 and 10^9 cells g^{-1}. In our simulations, we choose $\beta_\infty = 1$, which allows strong cell mortality by apoptosis, and $\overline{\beta} = 10^7$ and 10^8 cells g^{-1}. Finally the value of the sensitivity parameter n has almost no influence, as soon as it is large enough. In the simulations, we choose $n = 8$.

With values indicated in the second column of Table 1, we simulate Eq. (6) and the corresponding hematocrit, for the initial condition given by (15), and for $\overline{\beta} = 10^7$ and 10^8 cells g^{-1}. This is displayed in Fig. 4.

First note that when $\overline{\beta} = 10^8$ cells g^{-1}, the simulation gives very bad results, the curve does not fit experimental data at all, although this value of $\overline{\beta}$ would have been close to a realistic value. In fact, from (9) we know that the steady state E^* of the erythrocyte density verifies $E^* < AK/\gamma$. With values in Table 1, the quantity AK/γ equals 1.024×10^8 cells g^{-1}. Consequently, the erythrocyte density steady state E^* is almost always strictly less than $\overline{\beta} = 10^8$ cells g^{-1} (in fact as soon as $\tau_p > 0.05$ days, and more precisely for $\tau_p = 4$ days, $E^* = 7.39 \times 10^7$ cells g^{-1}), and progenitor apoptosis is thus strictly less than 50%. We are then in the presence of a slow behavior, the hematocrit reaching very slowly and smoothly its equilibrium value.

When $\overline{\beta} = 10^7$ cells g^{-1}, it appears that the hematocrit rapidly increases, as observed in experiments, but it does not reach very large values (the observed peak is about 52%, which does not belong to the acceptable range of values, determined by the standard deviation lines), and then the hematocrit smoothly reaches the steady state with no damped oscillations. Moreover, it is noticeable that the simulated peak occurs 6 days after the lowest hematocrit, whereas it occurs after 4–5 days in experiments. One can notice that the steady state of Eq. (6) equals, in this case, 1.03×10^7 cells g^{-1}, which is a rather low value (erythrocyte

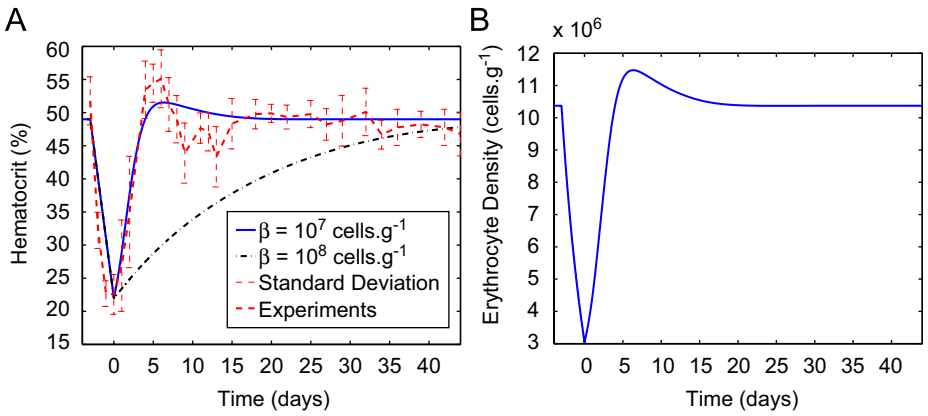

Fig. 4. Evolution of hematocrit over 44 days (Panel A), with values given in Table 1. The solid line corresponds to the simulation of Eq. (6) for $\overline{\beta} = 10^7$ cells g^{-1}, the dash-dotted one to the simulation of Eq. (6) for $\overline{\beta} = 10^8$ cells g^{-1}, and the dashed one to experimental results (average hematocrit, Fig. 1.A). Panel B: The solution $E(t)$ of Eq. (6) corresponding to the simulated hematocrit represented in A for $\overline{\beta} = 10^7$ cells g^{-1}. One can observe that the erythrocyte density converges quickly to the equilibrium $E^* = 1.03 \times 10^7$ cells g^{-1}. In both figures, simulations start at time $t = 0$, and initial conditions are drawn for $t<0$, as given in (15).

density in mice is usually considered to range between 10^8 and 3×10^8 cells g^{-1}). Due to (9) and the above remark, we know that the steady state E^* of the erythrocyte density cannot be very large in this model without self-renewal and, furthermore, with values in Table 1 it is less than 1.024×10^8 cells g^{-1}. Consequently, with this model, the estimated value of the erythrocyte density cannot be really biologically relevant since it will always be strictly less than 10^8 cells g^{-1}.

In Fig. 5, we have shown the solution $E(t)$ of Eq. (6), that is the erythrocyte evolution over time, when the Hopf bifurcation described by Proposition 1 occurs. The steady state is unstable in this case, which means that solutions of (6) oscillate about it. The steady state, at the bifurcation, equals 8.27×10^6 cells g^{-1}, which is still rather low. The erythrocyte density exhibits very long periods, of the order of 26 days.

One can also note that the Hopf bifurcation occurs for a large value of τ_p, so there is no hope to obtain damped oscillations for small—and so biologically relevant—values of τ_p. Thus it appeared to us that using apoptosis control as the only regulator of erythropoiesis results in a modelling unable to reasonably account for reality.

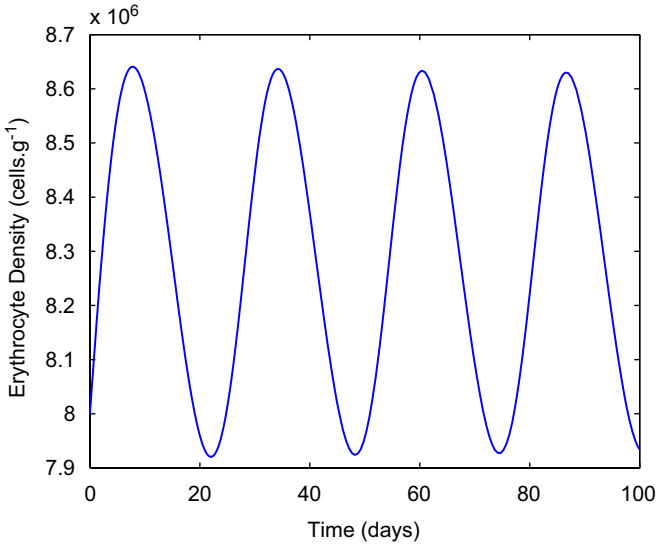

Fig. 5. The solution $E(t)$ of Eq. (6) when the Hopf bifurcation occurs, that is all parameters are given in Table 1 except $\tau_p = 14$ days. The erythrocyte number periodically oscillates with a period of about 26 days.

6. Influence of self-renewal

We now return to the analysis of system (4), that is we take progenitor self-renewal in erythropoiesis into consideration. Since glucocorticoids negatively mediate self-renewal, we choose the rate of self-renewal σ as a Hill function, that is a smooth decreasing function of the erythrocyte density E,

$$\sigma(E) = \sigma_0 \frac{\overline{\sigma}^m}{\overline{\sigma}^m + E^m}, \tag{16}$$

with $\sigma_0 > 0$ the maximum self-renewal rate, $\overline{\sigma} > 0$ the threshold value for which σ reaches half of its maximum value, and $m > 0$ the sensitivity of the self-renewal rate.

It can be noticed that no data are available in the literature to determine the shape of the self-renewal function (even though one would like to make this rate directly dependent on glucocorticoid concentrations). Hence, we chose to model it with a Hill function for one main reason. This kind of function is usually used in modelling kinase cascades reactions (Ferrell, 1996,1997), these latter being hidden behind our modelling approach. Hill functions have been used several times to model negative feedbacks at the stem cell level (Mackey, 1978; Pujo-Menjouet and Mackey, 2004). As explained below, coefficients of the self-renewal function (16) are then determined by trying to obtain the best fitting with experimental data.

A theoretical analysis of system (4) would be rather difficult and remains an open question, due to the presence

of multiple delays and nonlinearities. Hence, we focus our study on a numerical analysis of (4), trying to fit the data in Fig. 1.

Our first comment deals with parameters values used in the simulations of Eq. (6). As mentioned in the previous section, in order to finely fit experimental data, we sometimes chose unrealistic values of some parameters for the simulations of the model without self-renewal. For example, the value of $\overline{\beta}$ can be considered too small, when $\overline{\beta} = 10^7\,\text{cells}\,\text{g}^{-1}$, in comparison with the expected value of the erythrocyte steady state E^* (about $10^8\,\text{cells}\,\text{g}^{-1}$). One consequence was then an underestimation of the value of E^* in the model without self-renewal.

Consequently, we try here to adjust values of the parameters to experimentally known data of erythropoiesis. In particular (see Table 1), we only consider $\overline{\beta} = 10^8\,\text{cells}\,\text{g}^{-1}$.

All values we use in numerical simulations of system (4) are listed in Table 1, second column. In particular, we assume progenitors self-renew within one day (so $\tau_c = 1$ day). Values of coefficients that appear in the model without self-renewal are not modified, so we refer the reader to the previous section for our choices. Let us then focus ourselves on the values of the self-renewal rate.

Let us assume a maximum self-renewal rate of about $0.5\,\text{d}^{-1}$. This may seem small in comparison with the maximum apoptosis rate. Yet numerical simulations indicate that larger rates lead to overproduction of erythrocytes, self-renewal being more powerful than apoptosis in this case (this is not shown here). To maintain some balance between apoptosis and self-renewal, the value of $\overline{\sigma}$ must be chosen larger than $\overline{\beta}$. Note that this balance seems to be necessary because if one of the two controls was always more important than the other, then this latter would be useless in the model. We have observed in the last section that taking only apoptosis into account as a control for erythropoiesis gave not satisfactory results. The same conclusions occur if self-renewal is the only control. It seems that this condition adjusts, in some sense, the fact that the maximum apoptosis rate β_∞ is larger than the maximum self-renewal rate σ_0. So we choose $\overline{\sigma} = 10^9\,\text{cells}\,\text{g}^{-1}$. The sensitivity m of the self-renewal rate (16) is set to be $m = 5$. Similarly to the sensitivity of the apoptosis rate, it has almost no influence as soon as it is large enough.

Numerical simulations of system (4) with values indicated in Table 1 are displayed in Fig. 6. One can observe that the simulated curve does not exactly fit the experimental curve in Fig. 1A even though it exhibits more interesting features than the simulations in Fig. 4. In particular, there is a rapid increase of the hematocrit, following anemia, that reaches a peak (with a rather overestimated value about 57%, even though it could be acceptable), and then the hematocrit oscillates about the steady hematocrit, with damped oscillations, in contrast to the case without self-renewal where oscillations were not observed. Yet, periods of the oscillations are too large (about 30 days) and do not fit experimental data.

Adding progenitor self-renewal in our erythropoiesis modelling seems to affect the erythrocyte density evolution over time, but not in a sufficiently realistic way: the model does not give a correct answer of the hematocrit to a severe anemia, even though it exhibits interesting properties.

However, when increasing erythrocyte mortality rate γ, one can obtain a much more realistic simulation (see Fig. 7). The value of γ used in previous simulations describes an average lifetime of 40 days in mice. Yet this value must be understood as a normal mortality rate, that is in normal circumstances. Since we simulate a severe anemia, it is not realistic to keep the same value for the mortality of erythrocytes. Indeed, the anemia is obtained by injecting mice with phenylhydrazine and one effect of this substance is to dramatically alter the lifespan of erythrocytes (see Shimada, 1975 for a study on chicken's erythrocytes lifespan under induced anemia). One can see that the simulation of model (4) gives better results when changes in

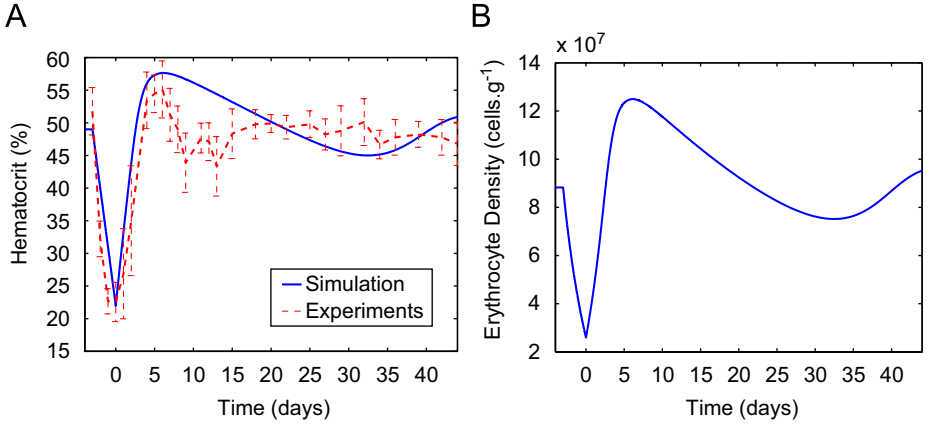

Fig. 6. Evolution of hematocrit over 44 days (Panel A), with values given in Table 1. The solid line corresponds to the simulation of the erythrocyte equation in system (4), and the dashed one to experimental results. Panel B: The solution $E(t)$ of system (4) corresponding to the simulated hematocrit represented in A. One can observe that the erythrocyte density oscillates about its equilibrium $E^* = 8.83 \times 10^7\,\text{cells}\,\text{g}^{-1}$. In both figures, simulations start at time $t = 0$, and initial conditions are drawn for $t < 0$, as given in (15).

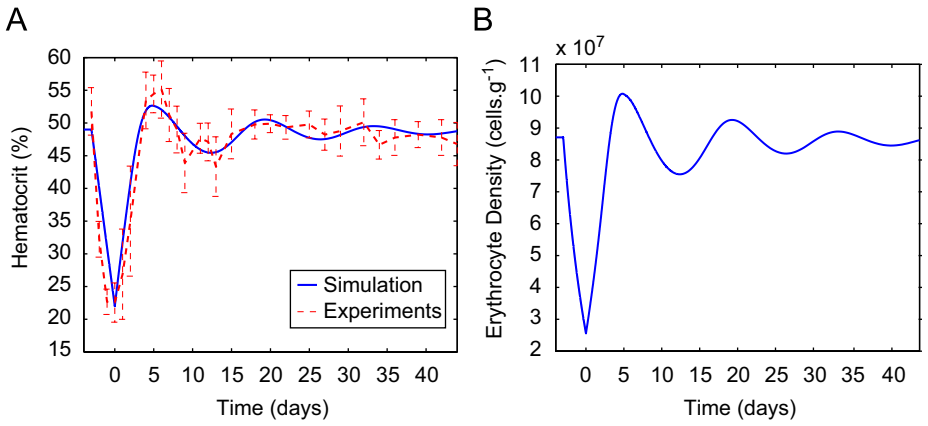

Fig. 7. Evolution of hematocrit over 44 days (Panel A), with values given in Table 1, except $\gamma = 0.15\,\mathrm{d}^{-1}$. The solid line corresponds to the simulation of the erythrocyte equation in system (4), and the dashed one to experimental results (Fig. 1.A). Panel B: The solution $E(t)$ of system (4) corresponding to the simulated hematocrit represented in A. One can observe that the erythrocyte density oscillates about its equilibrium $E^* = 8.7 \times 10^7\,\mathrm{cells\,g}^{-1}$. In both figures, simulations start at time $t = 0$, and initial conditions are drawn for $t<0$, as given in (15).

erythrocytes mortality are taken into account. Moreover, the steady state value E^* of the erythrocytes is in this case about $8.7 \times 10^7\,\mathrm{cells\,g}^{-1}$, which is a reasonable value.

One may object that the increase of the mortality rate γ could allow to obtain better results than the ones presented in Section 5.3 when simulating the model (6). However, and even though simulations are not shown here, this does not improve the model without self-renewal (data not shown). When the threshold value $\overline{\beta}$ equals $10^8\,\mathrm{cells\,g}^{-1}$, simulations do not differ from the one in Fig. 4, and the steady state value E^* is too small, $E^* = 1.7 \times 10^7\,\mathrm{cells\,g}^{-1}$. For $\overline{\beta} = 10^7\,\mathrm{cells\,g}^{-1}$, the simulated curve better fits experimental data (damped oscillations are observed, but with small amplitudes, and the simulated curve does not reach the experimental peak), but values of the erythrocyte density become even less realistic, with a steady state value E^* about $8.3 \times 10^6\,\mathrm{cells\,g}^{-1}$.

One can note that the progenitor dynamics in erythropoiesis process have not really been investigated in this study, mainly because we focused on data related to the hematocrit. However, when simulating the erythrocyte density in system (4), or (5)–(6), one can compute as well the progenitor density. This is done in Fig. 8, for both cases with and without self-renewal. It appears that the equilibrium value of the progenitor density is larger under the action of self-renewal (about $1.1 \times 10^6\,\mathrm{cells\,g}^{-1}$ versus $1.6 \times 10^4\,\mathrm{cells\,g}^{-1}$ when there is no self-renewal), and progenitor population dynamics are more complex in this case, because of the action of a negative and a positive feedback. This might provide a way to further investigate the role of progenitor self-renewal.

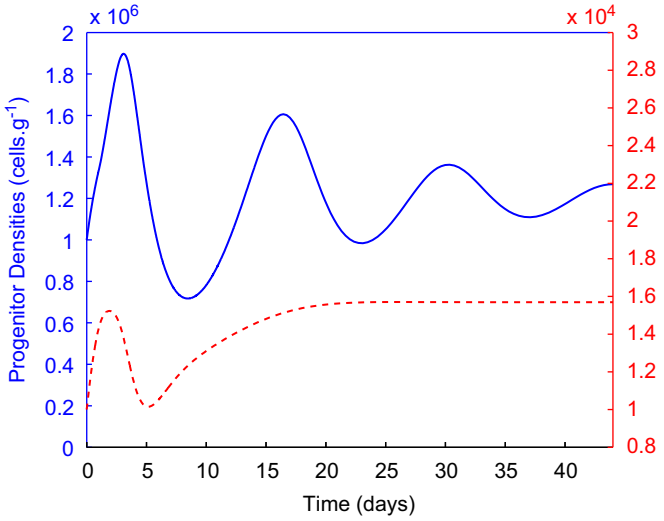

Fig. 8. Progenitors densities. The solid line is the progenitor density associated with the erythrocyte density in Fig. 7.B, that is in the model taking progenitor self-renewal into account, whereas the dashed line describes the evolution of progenitors without self-renewal (this population is associated with the erythrocyte density in Fig. 4.B). The scale of the solid line is set on the left vertical axis, and the scale of the dashed line on the right vertical axis. In particular, the equilibrium value of the progenitor density when self-renewal is incorporated in the model is about $1.1 \times 10^6\,\mathrm{cells\,g}^{-1}$, and about $1.6 \times 10^4\,\mathrm{cells\,g}^{-1}$ when there is no self-renewal.

7. Discussion

Based on recent advances in red blood cell research, we proposed a new mathematical model of erythropoiesis that takes into account up-to-date knowledge on red blood cells production—this means inhibition of apoptosis by EPO (Koury and Bondurant, 1990), and existence of erythroid progenitor self-renewal (Bauer et al., 1999; Gandrillon et al., 1999; Pain et al., 1991)—acquired at the cellular and molecular level these last few years.

Although hematopoietic stem cell dynamics are not considered in our study, the model incorporates two feedback loops, a negative glucocorticoid-mediated feedback of erythrocytes on progenitor self-renewal, and a positive EPO-mediated feedback on progenitor apoptosis. Even though this rendered the theoretical analysis of the complete model somewhat difficult, this proved to be

critical for obtaining a model that closely matches experimental data.

Moreover, as similarly done by Loeffler and Wichmann (1980), Wichmann and Loeffler (1985), Wichmann et al. (1985), or by Mackey (1978, 1979, 1997), Pujo-Menjouet and Mackey (2004), the model has been confronted to experimentally-obtained values in a non-equilibrium condition, that is here an experimentally induced severe anemia. We reasoned that our model should be able to model not only steady state but also stress erythropoiesis. This was especially needed since the role of glucocorticoids in mice has precisely been demonstrated to be critical for stress erythropoiesis (Bauer et al., 1999).

Although we could not derive all parameters values from the literature, we nevertheless were very careful to use only values that were within a biologically reasonable range. The fact that some variants of our model produced unreasonable quantitative values was clearly for us the sign that the modelling was not heading in the right direction. We tried to keep the number of parameters as small as possible, so that we could explore their influence on the results of the numerical situations.

Using this modelling strategy we could demonstrate that numerical simulations of the complete model, incorporating both a negative feedback of erythrocytes on progenitor self-renewal and a positive feedback on progenitor apoptosis, exhibited good results, the main characteristics of experimental data being well fitted by the model (see Section 6). These results tend to indicate that a correct modelling of erythropoiesis needs a clear understanding of the feedback mechanisms, in particular those that control progenitor populations (such as self-renewal).

The importance of a dynamically regulated and self-renewing stem cell population in hematopoiesis is self-evident as shown in numerous models, including Loeffler et al. (1989), Wichmann and Loeffler (1985), and Bernard et al. (2004) or Colijn and Mackey (2005a,b). Yet, we decided to deliberately omit this dynamical component in our model, essentially due to our ignorance of the precise molecular controls that could be involved in feedback controls of HSC populations, and of the cells from which the feedback could originate from (erythrocytes, or premature erythrocytes, could control HSC dynamics, among many other controls). On the contrary, molecular process controlling feedbacks on erythroid progenitors are rather well known, and this directed the modelling part of this work, allowing to go deeper in the analysis by investigating these molecular process and their precise roles in erythropoiesis. We are nevertheless aware that the experimental results we obtained might have been correctly modelled by a different model in which the self-renewing ability of hematopoietic stem cells would have been taken into account.

Note that this model makes two testable predictions:

(1) The first deals with the lifespan of mature cells. In order to get a perfect fitting we had to consider that the value of γ had to be severely reduced in the wake of phenylhydrazine injection. Since phenylhydrazine dramatically reduces the lifespan of erythrocytes, this might not seem to be far stretched. Nevertheless, this value can return to normal (1/40 per day) only after numerous days to capture the fading oscillations characteristic of our data. It would therefore be of great interest to measure the lifespan of the neosynthesized erythrocytes, after recovery and the following days. A reduction of lifespan can be predicted, since a study in a different species demonstrated that the red cells resulting from phenylhydrazine-induced anemia had a shorter life-span when compared to normal red cells (Berlin and Lotz, 1951, Nagai et al., 1968, 1971, Shimada, 1975, Stohlman, 1961). Such a change in life span could be due to specific membrane properties of the erythrocytes produced during stress erythropoiesis (Walter et al., 1975). In any case, this prediction could be tested in mice.
(2) The second type of predictions that can be made on the basis of our modelling is the behavior of the progenitor populations. Not only the absolute amount but also the oscillating behavior was quite different between the two versions of the model. Measuring the amount of progenitors of phenylhydrazine-treated mice could therefore confirm or not the necessity to incorporate erythroid progenitor self-renewal, and also lead to refinements of this model.

At least four perspectives from the modelling point of view can be drawn. We could first try to see up to which extent we could use the same model with different parameters values for modelling the appearance of erythroleukemia. It has for example been shown that an autocrine EPO production occurred in human erythroleukemia (Mitjavila et al., 1991). In our model this can be modelled quite simply by modifying the value of β. One could also try to analyze the influence of the self-renewal ability of our cells by modifying the value of σ. Reducing the amount of progenitors committing in a differentiation process, in order to model for example the effect of v-erbA oncogene on the differentiation process (Gandrillon, 2002), would require modifications of the model.

A second perspective of this work would be to dissect the feedback loops so as to incorporate explicitly important molecules like EPO receptors, signaling molecules and target genes. This would require a specific effort in multi-scale modelling. Thus a richer and more detailed model could be obtained without any loss in our modelling strategy, that is a model in which each parameter has a biological relevance, and in which the effect of each parameter on the blood cell population dynamics can be investigated.

It is obviously tempting to extend the model to more than one hematopoietic lineage. In order to keep the control of the model's behavior, one should start by modelling relatively simple lineage decisions. The lineage

choice between erythrocytic and megakaryocytic fate of a bipotent progenitor, thought to involve cross-antagonism between transcription factors (Starck et al., 2003), could represent an interesting step in this direction.

Finally, our model is a system of age-structured equations, and does not incorporate an explicit maturity-structured variable, that would describe cell differentiation. Hence, differentiation in this model is artificially introduced as an amplification parameter A, assumed to incorporate several divisions of progenitors. This leads to a limitation in the model, since progenitor self-renewal and differentiation processes are separated (first progenitor self-renew, and then they differentiate), although this decision is made at the single cell level. A way of considering differentiation explicitly is to add a discrete maturity variable (as it can be found in Adimy et al. (2007) and Bernard et al. (2003b)). This would lead to a system of several differential equations, each of them describing the dynamics of progenitors for a given maturity level. This could also bring more information on the dynamics of erythroid progenitors.

Altogether, our modelling scheme allowed us to design a model that fits experimental data well, allowing to make testable predictions, and that can be extended toward more hematopoietic lineages, in order to model, in the long run, a complete hematopoietic system. The success of our model was strictly dependent upon recent advances in our cellular and molecular understanding of red cell differentiation, and therefore its extension might require new advances, notably in the still open question of the feedback operating at the stem cell level by mature hematopoietic cells.

Acknowledgements

Authors are grateful to the anonymous referees for their helpful comments and suggestions that improved the revised version of this work. They also thank Prof. Michael C. Mackey for his comments and suggestions. We would like to thank all members of the BSMC group (http://bsmc.insa-lyon.fr) for stimulating discussions, Emmanuel Risler for his participation in early stages of this project, and Vitaly Volpert for his constant support during the shaping of the model. The work in Olivier Gandrillon's laboratory is supported by the Ligue contre le Cancer (Comité Départemental du Rhône), the UCBL, the CNRS, the Région Rhône Alpes and the Association pour la Recherche contre le Cancer (ARC). We are indebted to Edmund Derrington (CGMC UMR 5534) for his critical and thoughtful reading of the manuscript.

Appendix A. Method of the characteristics

We develop the method of the characteristics that allows us to express $p_{sr}(t,\tau_c)$ and $p(t,\tau_p)$ in terms of P and E, and then to give a clear expression of system (3).

Equations of the characteristics for system (1) are given by

$$\frac{da}{dt}=1,$$

from which we deduce $a(t)=t+a_0$, for $t\geqslant t_0=\max\{0,-a_0\}$. Then, setting

$$x(t)=p_{sr}(t,t+a_0),$$

we obtain from the second equation of (1)

$$\frac{dx}{dt}=-\beta(E(t))x(t).$$

Thus

$$x(t)=x(t_0)\exp\left(-\int_{t_0}^{t}\beta(E(s))\,ds\right).$$

If $t_0=0$, then

$$x(t)=x(0)\exp\left(-\int_{0}^{t}\beta(E(s))\,ds\right),$$

that is

$$p_{sr}(t,a)=p_{sr}(0,a-t)\exp\left(-\int_{0}^{t}\beta(E(s))\,ds\right)$$

if $t<a$,

and if $t_0=-a_0=t-a$, then

$$x(t)=x(t-a)\exp\left(-\int_{t-a}^{t}\beta(E(s))\,ds\right),$$

that is

$$p_{sr}(t,a)=p_{sr}(t-a,0)\exp\left(-\int_{t-a}^{t}\beta(E(s))\,ds\right)$$

if $a<t$.

In particular, we deduce, with (2), that

$$p_{sr}(t,\tau_c)=\sigma(E(t-\tau_c))P(t-\tau_c)\times\exp\left(-\int_{t-\tau_c}^{t}\beta(E(s))\,ds\right)\quad\text{for }\tau_c<t. \tag{A.1}$$

Similarly, we can obtain

$$p(t,a)=\begin{cases}p(t-a,0)\exp\left(-\int_{t-a}^{t}(\beta(E(s))+\sigma(E(s)))\,ds\right) & \text{if } a<t,\\ p(0,a-t)\exp\left(-\int_{0}^{t}(\beta(E(s))+\sigma(E(s)))\,ds\right) & \text{if } t<a,\end{cases}$$

so, from (2), for $a<t$,

$$p(t,a)=[K+2p_{sr}(t-a,\tau_c)]\times\exp\left(-\int_{t-a}^{t}(\beta(E(s))+\sigma(E(s)))\,ds\right).$$

It follows that, for $t>\tau_c$,

$$p(t,\tau_p)=[K+2p_{sr}(t-\tau_p,\tau_c)]\times\exp\left(-\int_{t-\tau_p}^{t}(\beta(E(s))+\sigma(E(s)))\,ds\right),$$

and for $t>\tau_p+\tau_c$, using (A.1) we obtain

$$p(t,\tau_p)=\left[K+2\sigma(E(t-\tau_p-\tau_c))P(t-\tau_p-\tau_c)\right.$$
$$\left.\times\ \exp\left(-\int_{t-\tau_p-\tau_c}^{t-\tau_p}\beta(E(s))\,\mathrm{d}s\right)\right]$$
$$\times\exp\left(-\int_{t-\tau_p}^{t}(\beta(E(s))+\sigma(E(s)))\,\mathrm{d}s\right). \qquad (A.2)$$

Hence, with expressions (A.1) and (A.2), we can write system (3), for $t>\tau_p+\tau_c$,

$$\begin{aligned}\frac{\mathrm{d}P}{\mathrm{d}t}(t)=&-[\beta(E(t))+\sigma(E(t))]P(t)\\&+K+2\sigma(E(t-\tau_c))P(t-\tau_c)\\&\times\exp\left(-\int_{t-\tau_c}^{t}\beta(E(s))\,\mathrm{d}s\right)\\&-\left[K+2\sigma(E(t-\tau_p-\tau_c))P(t-\tau_p-\tau_c)\right.\\&\left.\times\exp\left(-\int_{t-\tau_p-\tau_c}^{t-\tau_p}\beta(E(s))\,\mathrm{d}s\right)\right]\\&\times\exp\left(-\int_{t-\tau_p}^{t}(\beta(E(s))+\sigma(E(s)))\,\mathrm{d}s\right),\\ \frac{\mathrm{d}P_{sr}}{\mathrm{d}t}(t)=&-\beta(E(t))P_{sr}(t)+\sigma(E(t))P(t),\\&-\sigma(E(t-\tau_c))P(t-\tau_c)\\&\times\exp\left(-\int_{t-\tau_c}^{t}\beta(E(s))\,\mathrm{d}s\right),\\ \frac{\mathrm{d}E}{\mathrm{d}t}(t)=&-\gamma E(t)+A\exp\left(-\int_{t-\tau_p}^{t}(\beta(E(s))+\sigma(E(s)))\,\mathrm{d}s\right)\\&+\left[K+2\sigma(E(t-\tau_p-\tau_c))P(t-\tau_p-\tau_c)\right.\\&\left.\times\ \exp\left(-\int_{t-\tau_p-\tau_c}^{t-\tau_p}\beta(E(s))\,\mathrm{d}s\right)\right]. \qquad (A.3)\end{aligned}$$

One can easily check that the first and third equations in (A.3) do not depend on P_{sr}, so we omit the second equation in our study, and we focus on system (4).

Appendix B. Properties of complex eigenvalues

Let us study the existence and properties of purely imaginary roots of Eq. (12), in order to determine the local asymptotic stability of the unique steady state (P^*,E^*) of (5)–(6).

Let first check that $\lambda=0$ is not an eigenvalue of (10). Indeed, if $\lambda=0$ is an eigenvalue of (10), then from (12), we obtain

$$\gamma+\xi\tau_p=0,$$

which is impossible since $\gamma,\xi>0$ and $\tau_p\geqslant 0$.

Consequently, we can compute the integral in (12) and one can see that (12) is equivalent to

$$\lambda^2+\gamma\lambda+\xi-\xi\,\mathrm{e}^{-\lambda\tau_p}=0\quad\text{and}\quad\lambda\neq 0.$$

Then we focus on the study of complex roots of (13).

B.1. The case $\tau_p=0$

We first check that all roots of (13) have negative real parts when $\tau_p=0$, that is E^* is locally asymptotically stable in this case.

If $\tau_p=0$, Eq. (13) reduces to

$$\lambda^2+\gamma\lambda=0,$$

that is

$$\lambda(\lambda+\gamma)=0.$$

Since $\lambda=0$ is not a characteristic root of (10), we deduce that $\lambda=-\gamma<0$ is the only characteristic root, and since it is negative, we conclude to the local asymptotic stability of E^* when $\tau_p=0$.

B.2. Existence of purely imaginary eigenvalues

Assume $\tau_p>0$, and search for eigenvalues $\lambda=\mathrm{i}\omega$, with $\omega\in\mathbb{R}$. Then separating real and imaginary parts in (13), we obtain

$$\cos(\omega\tau_p)=1-\frac{\omega^2}{\xi}, \qquad (B.1)$$

$$\sin(\omega\tau_p)=-\frac{\gamma}{\xi}\omega. \qquad (B.2)$$

First note that if ω satisfies (B.1)–(B.2), then so does $-\omega$. Moreover, since $\lambda=0$ is not an eigenvalue of (10), we only focus on the existence of $\omega>0$ satisfying (B.1)–(B.2).

By summing the squares of both sides of (B.1)–(B.2), we obtain

$$\frac{\omega^2}{\xi^2}[\omega^2+\gamma^2-2\xi]=0.$$

Since we look for solutions $\omega>0$, this is equivalent to

$$\omega^2=2\xi-\gamma^2.$$

If $2\xi\leqslant\gamma^2$, then (10) has no purely imaginary characteristic roots, and so the stability of the steady state E^* cannot change. Since it is locally asymptotically stable when $\tau_p=0$, then it is locally asymptotically stable for $\tau_p\geqslant 0$ under condition $2\xi\leqslant\gamma^2$.

Now, let study the case $2\xi>\gamma^2$. From (11), this condition is equivalent to

$$E^*\beta'(E^*)>\frac{\gamma}{2}.$$

Under this condition, if (10) has purely imaginary roots $\pm\mathrm{i}\omega$, then $\omega=\sqrt{2\xi-\gamma^2}$. Therefore, from (B.1),

we deduce that

$$\cos\left(\tau_p\sqrt{2\xi-\gamma^2}\right)=\frac{\gamma^2}{\xi}-1,$$

that is

$$\tau_p=\frac{\arccos\left(\frac{\gamma^2}{\xi}-1\right)}{\sqrt{2\xi-\gamma^2}}.$$

Consequently, for $\tau_p=\tau_p^*:=\arccos(\gamma^2/\xi-1)/\sqrt{2\xi-\gamma^2}$, (10) has purely imaginary roots $\pm i\omega$, with $\omega=\sqrt{2\xi-\gamma^2}$.

B.3. Properties of purely imaginary roots

Let us show that purely imaginary roots $\pm i\omega^*:=\pm i\sqrt{2\xi-\gamma^2}$ of (10) that exist when $\tau_p=\tau_p^*$ are simple and satisfy the so-called *transversality condition*, that is

$$\frac{d\mathrm{Re}(\lambda(\tau_p^*))}{d\tau_p}>0.$$

Let consider a branch of eigenvalues $\lambda(\tau_p)$ of (13) such that

$$\lambda(\tau_p^*)=i\omega^*.$$

Then, from (13), it follows that

$$\lambda(\tau_p)^2+\gamma\lambda(\tau_p)+\xi-\xi e^{-\lambda(\tau_p)\tau_p}=0.$$

By differentiating the above equation with respect to τ_p, we obtain

$$[2\lambda(\tau_p)+\gamma+\xi\tau_p e^{-\lambda(\tau_p)\tau_p}]\frac{d\lambda}{d\tau_p}(\tau_p)+\xi\lambda(\tau_p)e^{-\lambda(\tau_p)\tau_p}=0. \tag{B.3}$$

By contradiction, assume $d\lambda(\tau_p^*)/d\tau_p=0$. Then from (B.3)

$$\xi i\omega^* e^{-i\omega^*\tau_p^*}=0,$$

that is, since $\xi>0$,

$$\omega^*\cos(\omega^*\tau_p^*)=0 \quad \text{and} \quad \omega^*\sin(\omega^*\tau_p^*)=0.$$

Since $\omega^*>0$, we deduce

$$\cos(\omega^*\tau_p^*)=0 \quad \text{and} \quad \sin(\omega^*\tau_p^*)=0,$$

which is equivalent, from (B.1)–(B.2), to

$$(\omega^*)^2=\xi>0 \quad \text{and} \quad \omega^*=0,$$

which is impossible. We conclude that $d\lambda(\tau_p^*)/d\tau_p\neq 0$ and $\pm i\omega^*$ are simple eigenvalues.

Moreover, from (13) and (B.3),

$$\begin{aligned}\left(\frac{d\lambda}{d\tau_p}(\tau_p^*)\right)^{-1}&=\frac{2\lambda(\tau_p^*)+\gamma+\xi\tau_p^* e^{-\lambda(\tau_p^*)\tau_p^*}}{-\xi\lambda(\tau_p^*)e^{-\lambda(\tau_p^*)\tau_p^*}}\\&=\frac{2\lambda(\tau_p^*)+\gamma}{-\xi\lambda(\tau_p^*)e^{-\lambda(\tau_p^*)\tau_p^*}}-\frac{\tau_p^*}{\lambda(\tau_p^*)}\\&=\frac{2i\omega^*+\gamma}{-i\omega^*[(i\omega^*)^2+\gamma(i\omega^*)+\xi]}-\frac{\tau_p^*}{i\omega^*}\\&=\frac{2i\omega^*+\gamma}{-i\omega^*[\xi-(\omega^*)^2+i\gamma\omega^*]}+i\frac{\tau_p^*}{\omega^*}.\end{aligned}$$

We deduce

$$\begin{aligned}&\left(\frac{d\lambda}{d\tau_p}(\tau_p^*)\right)^{-1}\\&=\frac{2i\omega^*+\gamma}{\gamma(\omega^*)^2+i\omega^*[(\omega^*)^2-\xi]}+i\frac{\tau_p^*}{\omega^*}\\&=\frac{\gamma^2(\omega^*)^2-2(\omega^*)^2[\xi-(\omega^*)^2]+i\gamma\omega^*[\xi+2\omega^*-(\omega^*)^2]}{\gamma^2(\omega^*)^4+(\omega^*)^2[(\omega^*)^2-\xi]^2}\\&\quad+i\frac{\tau_p^*}{\omega^*}.\end{aligned}$$

Consequently

$$\begin{aligned}\mathrm{Re}\left(\frac{d\lambda}{d\tau_p}(\tau_p^*)\right)^{-1}&=\frac{\gamma^2(\omega^*)^2-2(\omega^*)^2[\xi-(\omega^*)^2]}{\gamma^2(\omega^*)^4+(\omega^*)^2[(\omega^*)^2-\xi]^2}\\&=\frac{\gamma^2-2\xi+2(\omega^*)^2}{\gamma^2(\omega^*)^2+[(\omega^*)^2-\xi]^2}\\&=\frac{\gamma^2-2\xi+2(2\xi-\gamma^2)}{\gamma^2(2\xi-\gamma^2)+[2\xi-\gamma^2-\xi]^2}\\&=\frac{2\xi-\gamma^2}{\xi^2}.\end{aligned}$$

We conclude that

$$\mathrm{Re}\left(\frac{d\lambda}{d\tau_p}(\tau_p^*)\right)^{-1}=\frac{2\xi-\gamma^2}{\xi^2}>0.$$

References

Ackleh, A.S., Banks, H.T., Deng, K., 2002. A finite difference approximation for a coupled system of nonlinear size-structured population. Nonlinear Anal. 50, 727–748.

Ackleh, A.S., Deng, K., Ito, K., Thibodeaux, J., 2006. A structured erythropoiesis model with nonlinear cell maturation velocity and hormone decay rate. Math. Biosci. 204, 21–48.

Adimy, M., Crauste, F., 2003. Global stability of a partial differential equation with distributed delay due to cellular replication. Nonlinear Anal. 54 (8), 1469–1491.

Adimy, M., Crauste, F., 2007. Modelling and asymptotic stability of a growth factor-dependent stem cells dynamics model with distributed delay. Discrete Continuous Dynamical Syst. Ser. B 8 (1), 19–38.

Adimy, M., Crauste, F., Pujo-Menjouet, L., 2005a. On the stability of a maturity structured model of cellular proliferation. Discrete Continuous Dynamical Syst. Ser. A 12 (3), 501–522.

Adimy, M., Crauste, F., Ruan, S., 2005b. A mathematical study of the hematopoiesis process with applications to chronic myelogenous leukemia. SIAM J. Appl. Math. 65 (4), 1328–1352.

Adimy, M., Crauste, F., Ruan, S., 2006a. Modelling hematopoiesis mediated by growth factors with applications to periodic hematological diseases. Bull. Math. Biol. 68 (8), 2321–2351.

Adimy, M., Crauste, F., Ruan, S., 2006b. Periodic oscillations in leukopoiesis models with two delays. J. Theor. Biol. 242, 288–299.

Adimy, M., Crauste, F., El Abdllaoui, A., 2007. Asymptotic behavior of a discrete maturity structured system of hematopoietic stem cells dynamics with several delays. Math. Modelling Nat. Phenom. 1 (2).

Adimy, M., Pujo-Menjouet, L., 2003. Asymptotic behaviour of a singular transport equation modelling cell division. Discrete Continuous Dynamical Syst. Ser. B 3, 439–456.

Banks, H.T., Cole, C.E., Schlosser, P.M., Hien, T., 2004. Modelling and optimal regulation of erythropoiesis subject to benzene intoxication. Math. Biol. Eng. 1 (1), 15–48.

Bauer, A., Tronche, F., Wessely, O., Kellendonk, C., Reichardt, H.M., Steinlein, P., Schutz, G., Beug, H., 1999. The glucocorticoid receptor is required for stress erythropoiesis. Genes Dev. 13, 2996–3002.

Bélair, J., Mackey, M.C., Mahaffy, J.M., 1995. Age-structured and two-delay models for erythropoiesis. Math. Biosci. 128, 317–346.

Berlin, N.I., Lotz, C., 1951. Life span of the red blood cell of the rat following acute hemorrhage. Proc. Soc. Exp. Biol. Med. 78, 788.

Bernard, S., Bélair, J., Mackey, M.C., 2003a. Oscillations in cyclical neutropenia: new evidence based on mathematical modeling. J. Theor. Biol. 223, 283–298.

Bernard, S., Pujo-Menjouet, L., Mackey, M.C., 2003b. Analysis of cell kinetics using a cell division marker: mathematical modeling of experimental data. Biophys. J. 84, 3414–3424.

Bernard, S., Bélair, J., Mackey, M.C., 2004. Bifurcations in a white-blood-cell production model. C.R. Biol. 327, 201–210.

Burns, F.J., Tannock, I.F., 1970. On the existence of a G_0 phase in the cell cycle. Cell Tissue Kinet. 19, 321–334.

Chappell, D., Tilbrook, P.A., Bittorf, T., Colley, S.M., Meyer, G.T., Klinken, S.P., 1997. Prevention of apoptosis in J2E erythroid cells by erythropoietin: involvement of JAK2 but not MAP kinases. Cell Death Differ. 4, 105–113.

Colijn, C., Mackey, M.C., 2005a. A mathematical model of hematopoiesis—I. Periodic chronic myelogenous leukemia. J. Theor. Biol. 237, 117–132.

Colijn, C., Mackey, M.C., 2005b. A mathematical model of hematopoiesis—II. Cyclical neutropenia. J. Theor. Biol. 237, 133–146.

Ferrell, J.E., 1996. Tripping the switch fantastic: how a protein kinase cascade can convert graded inputs into switch-like outputs. Trends Biochem. Sci. 21 (12), 460–466.

Ferrell, J.E., 1997. How responses get more switch-like as you move down a protein kinase cascade. Trends Biochem. Sci. 22 (8), 288–289.

Gandrillon, O., 2002. The v-erbA oncogene. Assessing its differentiation-blocking ability using normal chicken erythrocytic progenitor cells. Methods Mol. Biol. 202, 91–107.

Gandrillon, O., Schmidt, U., Beug, H., Samarut, J., 1999. TGF-beta cooperates with TGF-alpha to induce the self-renewal of normal erythrocytic progenitors: evidence for an autocrine mechanism. EMBO J. 18, 2764–2781.

Haurie, C., Dale, D.C., Mackey, M.C., 1998. Cyclical neutropenia and other periodic hematological diseases: a review of mechanisms and mathematical models. Blood 92, 2629–2640.

Haurie, C., Dale, D.C., Mackey, M.C., 1999. Occurrence of periodic oscillations in the differential blood counts of congenital, idiopathic and cyclical neutropenic patients before and during treatment with G-CSF. Exp. Hematol. 27, 401–409.

Koury, M.J., Bondurant, M.C., 1990. Erythropoietin retards DNA breakdown and prevents programmed death in erythroid progenitor cells. Science 248, 378–381.

Krause, D.S., 2002. Regulation of hematopoietic stem cell fate. Oncogene 21, 3262–3269.

Kuang, Y., 1993. Delay differential equations with applications in population dynamics. Mathematics in Science and Engineering, vol. 191. Academic Press, New York.

Lajtha, L.G., 1959. On DNA labeling in the study of the dynamics of bone marrow cell populations. In: Stohlman, Jr., F. (Ed.), The Kinetics of Cellular Proliferation. Grune and Stratton. New York, pp. 173–182.

Loeffler, M., Wichmann, H.E., 1980. A comprehensive mathematical model of stem cell proliferation which reproduces most of the published experimental results. Cell Tissue Kinet. 13, 543–561.

Loeffler, M., Pantel, K., Wulff, H., Wichmann, H.E., 1989. A mathematical model of erythropoiesis in mice and rats. Part 1. Structure of the model. Cell Tissue Kinet. 22, 13–30.

Lomb, N.R., 1976. Least-squares frequency analysis of unequally spaced data. Astrophys. Space Sci. 39, 447–462.

Mackey, M.C., 1978. Unified hypothesis of the origin of aplastic anaemia and periodic hematopoïesis. Blood 51, 941–956.

Mackey, M.C., 1979. Dynamic hematological disorders of stem cell origin. In: Vassileva-Popova, G., Jensen, E.V. (Eds.), Biophysical and Biochemical Information Transfer in Recognition. Plenum Press, New York, pp. 373–409.

Mackey, M.C., 1997. Mathematical models of hematopoietic cell replication and control. In: Othmer, H.G., Adler, F.R., Lewis, M.A., Dallon, J.C. (Eds.), The Art of Mathematical Modelling: Case Studies in Ecology, Physiology and Biofluids. Prentice-Hall, Englewood Cliffs, NJ, pp. 149–178.

Mackey, M.C., Rudnicki, R., 1994. Global stability in a delayed partial differential equation describing cellular replication. J. Math. Biol. 33, 89–109.

Mackey, M.C., Rudnicki, R., 1999. A new criterion for the global stability of simultaneous cell replication and maturation processes. J. Math. Biol. 38, 195–219.

Mahaffy, J.M., Belair, J., Mackey, M.C., 1998. Hematopoietic model with moving boundary condition and state dependent delay: applications in erythropoiesis. J. Theor. Biol. 190, 135–146.

Mitjavila, M.T., Le Couedic, J.P., Casadevall, N., Navarro, S., Villeval, J.L., Dubart, A., Vainchenker, W., 1991. Autocrine stimulation by erythropoietin and autonomous growth of human erythroid leukemic cells in vitro. J. Clin. Invest. 88 (3), 789–797.

Nagai, K., Oue, K., Kawagoe, H., 1968. Studies on the short-lived reticulocytes by use of the in vitro labeling method. Acta. haematol. Jpn 31, 967.

Nagai, K., Ishizu, K., Kakishita, E., 1971. Studies on the erythroblast dynamics based on the production of fetal hemoglobin. Acta Haematol. Jpn. 34.

Pain, B., Woods, C.M., Saez, J., Flickinger, T., Raines, M., Kung, H.J., Peyrol, S., Moscovici, C., Moscovici, G., Jurdic, P., Lazarides, E., Samarut, J., 1991. EGF-R as a hemopoietic growth factor receptor: the c-erbB product is present in normal chicken erythrocytic progenitor cells and controls their self-renewal. Cell 65, 37–46.

Pantel, K., Loeffler, M., Bungart, B., Wichmann, H.E., 1990. A mathematical model of erythropoiesis in mice and rats. Part 4. Differences between bone marrow and spleen. Cell Tissue Kinet. 23, 283–297.

Pujo-Menjouet, L., Bernard, S., Mackey, M.C., 2005. Long period oscillations in a G_0 model of hematopoietic stem cells. SIAM J. Appl. Dynamical Syst. 4 (2), 312–332.

Pujo-Menjouet, L., Mackey, M.C., 2004. Contribution to the study of periodic chronic myelogenous leukemia. C.R. Biol. 327, 235–244.

Roeder, I., 2006. Quantitative stem cell biology: computational studies in the hematopoietic system. Curr. Opinion Hematol. 13, 222–228.

Roeder, I., Loeffler, M., 2002. A novel dynamic model of hematopoietic stem cell organization based on the concept of within-tissue plasticity. Exp. Hematol. 30, 853–861.

Sakata, S., Enoki, Y., Tomita, S., Kohzuki, H., 1985. In vitro erythropoietin assay based on erythroid colony formation in fetal mouse liver cell culture. Br. J. Haematol. 61 (2), 293–302.

Shampine, L.F., Thompson, S., 2001. Solving DDEs in MATLAB. Appl. Numer. Math. 37, 441–458. doi:10.1016/S0168-9274(00)00055-6. ⟨http://www.radford.edu/thompson/webddes/⟩.

Shimada, A., 1975. The maturation of reticulocytes. II Life-span of red cells originating from stress reticulocytes. Acta Med. Okayama 29 (4), 283–289.

Starck, J., Cohet, N., Gonnet, C., Sarrazin, S., Doubeikovskaia, Z., Doubeikovski, A., Verger, A., Duterque-Coquillaud, M., Morle, F., 2003. Functional cross-antagonism between transcription factors FLI-1 and EKLF. Mol. Cell Biol. 23 (4), 1390–1402.

Stohlman, F., 1961. Humoral regulation of erythropoiesis. VII. Shortened survival of erythrocytes by erythropoietin or severe anemia. Proc. Soc. Exp. Biol. Med. 107, 884.

Walter, H., Krob, E.J., Ascher, G.S., 1975. Abnormal membrane surface properties during maturation of rat reticulocytes elicited by bleeding as measured by partition in two-polymer aqueous phases. Br. J. Haematol. 31 (2), 149–157.

Watt, F.M., Hogan, B.L., 2000. Out of Eden: stem cells and their niches. Science 287, 1427–1430.

Weissman, I.L., 2000. Stem cells: units of development, units of regeneration, and units in evolution. Cell 100, 157–168.

Wichman, H.E., Loeffler, M., 1985. Mathematical Modeling of Cell Proliferation. CRC Press, Boca Raton, FL.

Wichmann, H.E., Loeffler, M., Schmitz, S., 1985. A concept of hemopoietic regulation and its biomathematical realisation. Blood Cells 14, 411–429.

Wichmann, H.E., Loeffler, M., Pantel, K., Wulff, H., 1989. A mathematical model of erythropoiesis in mice and rats. Part 2. Stimulated erythropoiesis. Cell Tissue Kinet. 22, 31–49.

Wulff, H., Wichmann, H.E., Loeffler, M., Pantel, K., 1989. A mathematical model of erythropoiesis in mice and rats. Part 3. Suppressed erythropoiesis. Cell Tissue Kinet. 22, 51–61.